Universiteit Leiden
The Netherlands

The activation mechanisms of G protein-coupled receptors : the case of the adenosine A2B and HCA2/3 receptors

Liu, R.

Citation
Liu, R. (2016, December 8). *The activation mechanisms of G protein-coupled receptors : the case of the adenosine A2B and HCA2/3 receptors*. Retrieved from https://hdl.handle.net/1887/44797

Version:	Not Applicable (or Unknown)
License:	Licence agreement concerning inclusion of doctoral thesis in the Institutional Repository of the University of Leiden
Downloaded from:	https://hdl.handle.net/1887/44797

Note: To cite this publication please use the final published version (if applicable).

Cover Page

Universiteit Leiden

The handle http://hdl.handle.net/1887/44797 holds various files of this Leiden University dissertation

Author: Rongfang Liu
Title: The activation mechanisms of G protein-coupled receptors : the case of the adenosine A2B and HCA2/3 receptors
Issue Date: 2016-12-08

Chapter 3

A yeast screening method to decipher the interaction between the adenosine A_{2B} receptor and the C-terminus of different G protein α-subunits

This chapter is based upon:

Rongfang Liu, Nick J. A. Groenewoud, Miriam C. Peeters, Eelke B. Lenselink, Ad P. IJzerman

Purinergic Signalling ***2014*** *10: 441-453*

Abstract

The expression of human G protein-coupled receptors (GPCRs) in *Saccharomyces cerevisiae* containing chimeric yeast/mammalian G_{α} subunits provides a useful tool for the study of GPCR activation. In this study, we used a one-GPCR-one-G protein yeast screening method in combination with molecular modeling and mutagenesis studies to decipher the interaction between GPCRs and the C-terminus of different α-subunits of G proteins. We chose the human adenosine A_{2B} receptor ($hA_{2B}R$) as a paradigm, a typical class A GPCR that shows promiscuous behavior in G protein coupling in this yeast system. The wild-type $hA_{2B}R$ and five mutant receptors were expressed in 8 yeast strains with different humanized G proteins, covering the four major classes: $G_{\alpha i}$, $G_{\alpha s}$, $G_{\alpha q}$ and $G_{\alpha 12}$. Our experiments showed that a tyrosine residue (Y) at the C-terminus of the G_{α} subunit plays an important role in controlling the activation of GPCRs. Receptor residues $R103^{3.50}$ and $I107^{3.54}$ are vital too in G protein-coupling and the activation of the $hA_{2B}R$, whereas $L213^{IL3}$ is more important in G protein inactivation. Substitution of $S235^{6.36}$ to alanine provided the most divergent G protein coupling profile. Finally, $L236^{6.37}$ substitution decreased receptor activation in all G protein pathways, although to a different extent. In conclusion, our findings shed light on the selectivity of receptor/G protein coupling, which may help in further understanding GPCR signaling.

Introduction

G protein-coupled receptors (GPCRs), also known as seven-transmembrane receptors (7TMRs), are a major class of targets for many of today's medicines, to combat ailments such as inflammation, cardiac malfunction, asthma and cancer. Ligands interact with these transmembrane proteins in many different ways, intervening with or mimicking their activation process, which is mediated mostly by a heterotrimeric G protein, composed of α, β and γ subunits[1, 2]. However, the exact mechanism of GPCR activation at the molecular level is still largely unknown. Here, we used the $hA_{2B}R$, a typical class A GPCR, as a paradigm to decipher the interaction between receptors and their G proteins.

The adenosine receptors include four subtypes: A_1R, $A_{2A}R$, $A_{2B}R$ and A_3R, which have attracted much attention as therapeutic targets in recent years. All the adenosine receptors are ubiquitously expressed in the human body[3] and can target different intracellular signaling pathways by responding to the same endogenous ligand adenosine. The $A_{2B}R$ has the lowest affinity for adenosine[4] and has been less investigated than other adenosine receptors. Several studies have shown that blocking $A_{2B}R$ signaling reduces experimental autoimmune encephalomyelitis[5] and inhibits growth of prostate cancer cells[6], breast tumors[7] and bladder tumors[8, 9]. On the other hand, stimulation of $A_{2B}R$ protects against trauma-hemorrhagic shock-induced lung injury[10] , CHX-induced apoptosis[6] and also vascular injury[11].

Yeast can provide a powerful platform for studying GPCRs and their G protein coupling and selectivity. *Saccharomyces cerevisiae* (*S. cerevisiae*) strains, each expressing a specific human G_α/yeast Gpa1 protein chimera, have been used to express heterologous GPCRs, for instance in high-throughput screening assays for drug discovery[12], to perform random mutagenesis screening[13, 14], and to assess the preference of G_α pathways[15] and functional selectivity of agonists and antagonists[16-18]. Several lines of evidence indicate that the C-terminal five amino acid residues of a G protein are sufficient for coupling with many human receptors, including the $hA_{2B}R$[19]. One of the advantages of the yeast system used is that while these five amino acids of many human G protein α-subunits were

'transplanted' to replace these residues on the yeast's endogenous G protein, Gpa1p (see also Table 1), all other aspects of the system remain the same and intact[20, 21].

In the present study, we used this one-GPCR-one-G protein yeast screening method in combination with molecular modeling and mutagenesis studies. Our goal was to provide more information about the mechanism of activation of the $hA_{2B}R$ and the role the binding pocket for the G_{α} protein's C-terminus plays in that process. Our findings provide further evidence for the A_{2B} receptor's G protein preferences, which in itself may be useful for designing and screening selective agonists and antagonists for this receptor. At the same time, our findings have a broader relevance as they reflect on the GPCR-G protein interface.

Table 1. The genotypes of the yeast strains used for transformations[20, 21, 49].

Strain	Genotype	The five C-terminal residues of G_{α}
MMY11	**MATa** *his3 ade2 leu2 trp1 ura3 can1 fus1:: FUS1-HIS3 FUS1-lacZ::LEU2 farΔ::ura3Δgpa1Δ ::ADE2Δsst2Δ ::ura3Δste2Δ::G418^R*	
MMY12 ($G_{\alpha WT}$)	MMY11*TRP1::GPA1*	KIGII^{COOH}
MMY23 ($G_{\alpha i1}$)	MMY11*TRP1::Gpa1/*$G_{\alpha i1(5)}$	DCGLF^{COOH}
MMY24 ($G_{\alpha i3}$)	MMY11*TRP1::Gpa1/*$G_{\alpha i3(5)}$	ECGLY^{COOH}
MMY28 ($G_{\alpha s}$)	MMY11*TRP1::Gpa1/*$G_{\alpha s(5)}$	QYELL^{COOH}
MMY14 ($G_{\alpha q}$)	MMY11*TRP1::Gpa1/*$G_{\alpha q(5)}$	EYNLV^{COOH}
MMY21 ($G_{\alpha 14}$)	MMY11*TRP1::Gpa1/*$G_{\alpha 14(5)}$	EFNLV^{COOH}
MMY19 ($G_{\alpha 12}$)	MMY11*TRP1::Gpa1/*$G_{\alpha 12(5)}$	DIMLQ^{COOH}
MMY20 ($G_{\alpha 13}$)	MMY11*TRP1::Gpa1/*$G_{\alpha 13(5)}$	QLMLQ^{COOH}

Materials and methods

hA_{2B} Receptor/G protein homology modeling

A homology model was created using Molsoft's ICM Homology tool (Version 3.7-2)[22]. The β_2 adrenergic receptor (β_2AR) in complex with the G_s protein[23] (PDB: 3SN6) was chosen as template since it was the closest (and currently only) homolog of the $hA_{2B}R$ containing the $G_{\alpha s}$ protein, with 30% sequence identity and 48% sequence similarity using a pair-wise sequence alignment method (EMBOSS_matcher; http://www.ebi.ac.uk/Tools/psa/emboss_matcher/). The $hA_{2B}R$ sequence (uniprot: P29275) was modeled onto 3SN6 and residues were selected to be individually mutated to alanine based on the following two criteria: 1) within *5 Å* distance from the last five amino acids of the $G_{\alpha s}$ protein (QYELL) and 2) oriented towards the $G_{\alpha s}$ protein. Final visualizations were created using PyMOL (The PyMOL Molecular Graphics System, Version 1.5.0.4 Schrödinger, LLC)[24].

Generation of point mutations

The S. *cerevisiae* expression vectors, the pDT-PGK and pDT-PGK_A_{2B} receptor plasmids, were kindly provided by Dr. Simon Dowell from GSK (Stevenage, UK). The DNA primers of the mutants of the A_{2B} receptor were designed by the QuikChange® Primer Design Program on the website of Agilent Technologies, and contained a single substitution resulting in a codon change for the desired amino acid substitution. The reverse primer sequence of each mutant was the reverse complement of the forward primer. These primers and their complements were synthesized (Eurogentec, the Netherlands) and then used to generate mutant plasmids according to the QuikChange method from Stratagene. The mutagenic reaction contained 40 ng of the pDT-PGK_A_{2B} construct plasmid as dsDNA template, 10 μM of each primer, 1 μl of dNTP mix, 2.5 μl of 10× reaction buffer and 2.5 U *PfuUltra* HF DNA polymerase. The following thermal cycling parameters were used in the PCR apparatus (T100™ Thermal Cycler, BIO-RAD): 95 °C for 30 s, 55 °C for 1 min, and 68 °C for 10 min. The number of mutagenic PCR cycles was set to 20. Methylated or hemimethylated non-mutated plasmid

DNA was removed by adding 5 U *Dpn* I restriction enzyme for 2 h at 37 °C. The mutated DNA products were transformed into XL-1 Blue supercompetent cells and other details were according to the manual of the QuikChange® II Site-Directed Mutagenesis Kit. Mutant plasmids were isolated from a single clone using a QIAprep midi plasmid purification kit (QIAGEN, the Netherlands). The mutants were confirmed by DNA sequencing (LGTC, Leiden, the Netherlands).

Transformation in *S. cerevisiae* strains

Each mutant plasmid was transformed according to the Lithium-Acetate procedure[25] into a panel of engineered *S. cerevisiae* yeast strains expressing different Gpa1p/G_{α} chimeras. The yeast strains were derived from the MMY11 strain and further adapted to communicate with mammalian GPCRs. The difference between these integrated Gpa1p/G_{α} chimeras is that the last five amino acids of the endogenous Gpa1p C-terminus have been replaced with the same sequence as that from mammalian G_{α} proteins[20, 21] (Table 1). To measure the signaling of GPCRs, the pheromone signaling pathway of these strains was coupled via the *FUS1* promoter to *HIS3* (imidazoleglycerol-phosphate dehydratase), an enzyme catalyzing the sixth step in histidine biosynthesis to produce histidine. 3-AT (3-amino-[1, 2, 4]- triazole), a competitive inhibitor of imidazoleglycerol-phosphate dehydratase, was added to the assay to reduce background activity caused by endogenous histidine[20]. The degree of receptor activation induced by an agonist of the GPCR was measured by the growth rate of the yeast on histidine-deficient medium.

Liquid growth assay

To measure the efficiency of GPCR-G protein coupling, concentration-growth curves were generated in a liquid growth assay[26]. This assay was carried out in 96-well plates and the growth was determined by measuring the absorption at a wavelength of approx. 600 nm (OD_{600}). To set up an assay, cells were grown to saturation selecting for the transformed plasmid, then seeded at low cell density (2×10^4 cells/ml) into assay medium (YNB + adenine + tryptophan + 10mM 3-AT) lacking histidine and dispensed into assay plates containing the adenosine

receptor agonist NECA (10^{-9} – 10^{-4} M). The 96-well plate was then incubated for 35 h at 30 °C in a Genios plate reader (Tecan, Durham, NC), keeping the cells in suspension by shaking every 10 min at 300 rpm for 1 min. Results were obtained from two independent experiments, performed in duplicate. EC_{50} values and E_{max} values of the liquid assay were analyzed using the nonlinear regression package available in Prism 5.0 software (GraphPad Software Inc., San Diego, CA, USA).

Whole cell radioligand binding experiments

Yeast cells from an overnight culture expressing the wild-type or mutated $hA_{2B}R$ were harvested from rich YAPD medium by centrifuging 2,000 *g* for 5 min. The pellet of cells was washed once with 0.9% NaCl. The cells were centrifuged again using the same speed and diluted in the assay buffer (50 mM Tris-HCl pH7.4 + 1 mM EDTA) to OD_{600} = 40 (OD_{600} = 1 ≈ 2.5×10^7 cells/ml). Binding experiments were performed with 1.5 nM of the A_{2B} receptor selective antagonist [^{3}H]PSB-603, and a final cell concentration of 25×10^7 cells/ml in a total volume of 100 µl. Nonspecific binding (NSB) was determined by additionally adding NECA at a final concentration of 1 mM. Samples were incubated for 1 h at 25 °C keeping the cells in suspension by shaking vigorously. 1 ml of ice-cold assay buffer was added to samples to terminate incubation and the samples were harvested on a Millipore manifold with GF/B filters pre-incubated in 0.1% polyethylenimine (PEI) at a pressure of 200 mbar, to separate free from receptor-bound radioligand by washing twice with 2 ml buffer (50 mM Tris-HCl pH7.4 + 1 mM EDTA + 0.1%BSA). The filters were transferred into mini-vials and 3.5 ml of PerkinElmer Emulsifier Safe was added, and subsequently incubated for at least 2 h. Filter-bound radioactivity was determined as counts per minute by scintillation spectrometry (Tri-Carb 2900TR; PerkinElmer Life and Analytical Sciences). Results were obtained from at least three independent experiments, performed in duplicate.

Preparation of yeast protein extractions and immunoblotting

Protein extractions were performed with trichloroacetic acid (TCA) according to

the Clontech Yeast Protocols Handbook 2001. Yeast transformants were grown in 2 ml YAPD medium and were harvested in mid-exponential phase (1.2×10^8 cells). The yeast cells were collected and washed with cold water. Subsequently the yeast cells were broken by vigorous vortexing with 20% TCA and glass beads. The broken yeast cells and the glass beads were washed twice with 200 µl 5% TCA and centrifuged at 3,000 rpm for 2 minutes. The supernatant was collected and centrifuged again at 6,000 rpm for 2 minutes. The pellets were resuspended with cold SDS/PAGE loading buffer (100 mM EDTA, 1 M Tris, 10% SDS, 0.5% Bromophenol blue) and 1 M Tris was added to neutralize all remaining TCA. The samples were incubated for 30 min at 37 °C and centrifuged again at 2,000 rpm for 10 min.

Each sample of 4 µl containing 24 µg protein was loaded on 12.5% SDS/PAGE gel and then blotted on Hybond-ECL membranes (GE Healthcare, the Netherlands) using a semi-automated electrophoresis technique (PhastSystem™, Amersham Pharmacia Biotech). The Hybond-ECL membranes were blocked with TBS containing 5% milk powder for 1 h and washed three times with TBST (0.05% Tween-20, TBS pH 7.6). The membranes were incubated with 1:1250 diluted rabbit anti-human A_{2B} receptor antibody for 1 h. This antibody was directed against the C-terminal region of the $A_{2B}R$ and was kindly provided by Dr. I. Feoktistov (Vanderbilt University, Nashville)[27]. After thorough removal of unbound antibody from the membranes by washing three times with TBST, the membranes were incubated with 1:2,500 diluted HRP-conjugated goat anti-rabbit IgG (Jackson ImmunoResearch Laboratories) for 1 h. The membranes were washed twice with TBST and once with TBS. The specific signal of the A_{2B} receptor was probed according to the ECL Western blotting analysis system (GE Heathcare, the Netherlands) using enhanced chemiluminescence (ChemiDox XRS, BIO-RAD). The nonspecific band at approx. 45 kDa was used as loading control and the specific $hA_{2B}R$ protein bands were at 29 kDa and 48 kDa. The ratio was determined between the density of the specific bands and density of the nonspecific band that was always present on the blots. MMY12 carrying wild-type or mutant receptor was set as 100% and MMY12 carrying the empty vector pDT-PGK without receptor was set as 0%.

Results

G protein selectivity of the wild-type hA_{2B} receptor

To investigate the activation mechanism of the hA_{2B} receptor at the interface of the C terminus of the G protein G_{α} subunit, we expressed the yeast plasmid pDT-PGK_hA_{2B}R in a panel of eight yeast *S. cerevisiae* strains with humanized G proteins. Corresponding to the replaced last five C-terminal residues of the mammalian G_{α} subunit, they were classified into five families: $G_{\alpha WT}$ (MMY12), $G_{\alpha s}$ (MMY28), $G_{\alpha i}$ (MMY23 and MMY24), $G_{\alpha 12}$ (MMY19 and MMY20), and $G_{\alpha q}$ (MMY14 and MMY21) (Table 1)[19]. When the expressed hA_{2B} receptor is activated by an agonist, the yeast pheromone signalling pathway is activated through a chimeric yeast/mammalian G protein leading to subsequent transcription of the HIS3 reporter gene and consequently histidine production[28]. Subsequent growth of the yeast cells on histidine-deficient medium was determined by measuring the absorption at a wavelength of 595 nm, which reflects the activation of the expressed receptor by the adenosine receptor agonist NECA. Concentration-response curves of NECA on the wild-type receptor in MMY28($G_{\alpha s}$), MMY24($G_{\alpha i3}$), MMY12($G_{\alpha WT}$), MMY19($G_{\alpha 12}$) and MMY14($G_{\alpha q}$) are shown in Figure 1 and the values of EC_{50}, and E_{max} of all strains are shown in Table 2.

We found the five humanized different G protein pathways MMY28($G_{\alpha s}$), MMY24($G_{\alpha i3}$), MMY21($G_{\alpha 14}$), MMY23($G_{\alpha i1}$) and MMY20($G_{\alpha 13}$) to show varying degrees of enhancement compared to the coupling efficiency of the wild-type hA_{2B}R in the wild-type yeast G_{α} strain MMY12($G_{\alpha WT}$). The most efficient yeast strain MMY28($G_{\alpha s}$) showed a significant 15-fold improvement in coupling efficiency and also MMY24($G_{\alpha i3}$) showed a significant 6.5-fold enhancement in coupling efficiency. Two strains, MMY14($G_{\alpha q}$) and MMY19($G_{\alpha 12}$), responded less to NECA, with significantly higher EC_{50} values for this agonist. In terms of intrinsic activity (E_{max} values) there was little difference between the strains, however. The one exception was in MMY28($G_{\alpha s}$) with a large degree of constitutive activity (approx. 30% of the maximal response of MMY12 in response to the agonist NECA (10^{-4} M). This may be a feature of the MMY28 strain itself since expression of plasmid pDT-PGK (without any receptor) yielded a similar degree

of constitutive activity (data not shown).

Bioinformatics and Molecular Modeling

To further decipher the interaction between the $hA_{2B}R$ and G proteins, we predicted a number of amino acid residues as important for activation of G proteins from $hA_{2B}R$ homology modeling. There are more than 75 crystal structures of 18 different class A GPCRs now[29], however, only two receptors, β_2AR and opsin (Ops), have been cocrystallised with the $G_{\alpha s}$ protein[23] and an 11 amino acid synthetic peptide of $G_{\alpha t}$[30], respectively. The β_2AR-G_s crystal structure (PDB: 3SN6) was chosen as template for mapping amino acid residues of $hA_{2B}R$ that are involved in G protein activation. The $h\beta_2$AR shares 30% sequence identity with the $hA_{2B}R$ (Fig. 2A), compared to 23% homology with bovine opsin. In many mammalian cells, the $hA_{2B}R$ prefers to couple to G_s next to G_q proteins[31], another indication of the validity of this particular homology modeling approach. The model predicted 16 amino acids to interact with $G_{\alpha s}$ (i.e. with QYELL, the last five amino acid residues of it): $D102^{3.49}$, $R103^{3.50}$, $A106^{3.53}$, $I107^{3.54}$, $Y113^{3.60}$, $I205^{5.61}$, $A209^{5.65}$, $Q212^{IL3}$, $L213^{IL3}$, $R215^{IL3}$, $H231^{6.32}$, $A232^{6.33}$, $S235^{6.36}$, $L236^{6.37}$, $R293^{8.46}$, $N294^{8.47}$.

Arginine (R) $103^{3.50}$, isoleucine (I) $107^{3.54}$, leucine (L) 213^{IL3}, serine (S) $235^{6.36}$ and leucine (L) $236^{6.37}$ were selected for mutation into alanine as they are both closest to the $G_{\alpha s}$ protein and with their side chains oriented towards the $G_{\alpha s}$ protein as well (Fig. 2B). These selected five residues are also shown in the snake plot of the $hA_{2B}R$ (Fig. 2C). $R103^{3.50}$ and $I107^{3.54}$ are located on the intracellular side of TM3 and are included in the consensus sequence $(I/L)XXDR^{3.50}YXX(I/V)^{3.54}$[32]. $R^{3.50}$ is a part of the most conserved motif in the class A GPCRs: Asp-Arg-Tyr (DRY). The residues on positions 3.50, 3.54 and 6.36 according to Ballesteros-Weinstein numbering[33] are also conserved as part of the G protein-binding region in the bovine opsin-G_t peptide crystal structure[23, 29, 30].

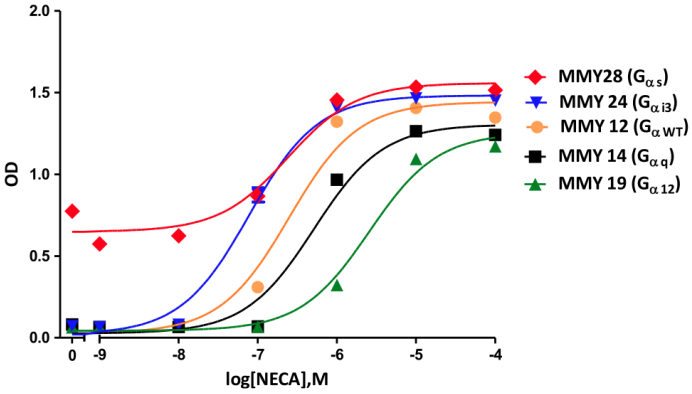

Fig. 1 Concentration-effect curves from liquid assay experiments are shown of the A_{2B} wild-type receptor in MMY28 ($G_{\alpha s}$), MMY24 ($G_{\alpha i3}$), MMY12 ($G_{\alpha WT}$), MMY14 ($G_{\alpha q}$) and MMY19 ($G_{\alpha 12}$) responding to the adenosine receptor agonist NECA. The assay was performed in YNB-ULH medium.

G protein coupling profiles of five mutant A_{2B} receptors

To assess the function of these five residues in G protein activation, we performed a functional yeast liquid assay to determine whether the G protein activation profiles of these mutants had changed or not. NECA concentration-response curves revealed that all five single amino acid changes in the receptor resulted in substantially different humanized G protein coupling profiles of the $hA_{2B}R$ (Table 2; Fig. 3).

The $R103^{3.50}A$ receptor failed to couple to all humanized G protein pathways except for MMY28($G_{\alpha s}$) with a comparable EC_{50} value, only 2-fold higher than wild-type receptor (Table 2). Mutant receptor $I107^{3.54}A$ only responded with higher than wild-type EC_{50} values for NECA of 7629 nM to MMY23($G_{\alpha i1}$) with a reduced E_{max} value of 37%, and 47 nM to MMY28($G_{\alpha s}$) with a maximal activation level. Other humanized G protein pathways did not respond to NECA anymore (Table 2).

A

```
A2B              11 VALELVIAALSVAGNVLVCAAVGTANTLQTPTNYFLVSLAAADVAVGLFA     60
                    :.:.|::.|: |.|||||..|:.....|||.||||:.|||.||:.:||..
beta2            38 IVMSLIVLAI-VFGNVLVITAIAKFERLQTVTNYFITSLACADLVMGLAV     86

A2B              61 IPFAITISLGFCTDF--YGCLFLACFVLVLTQSSIFSLLAVAVDRYLAIC     108
                    :||.....|.....|  :.|.|.....::...:||.:|..:|||||.|||.
beta2            87 VPFGAAHILMKMWTFGNFWCEFWTSIDVLCVTASIETLCVIAVDRYFAIT     136

A2B             109 VPLRYKSLVTGTRARGVIAVLWVLAFGIGLTPF-LGW-NSKDSATNNCTE     156
                    .|.:|:||:|..:||.:|.::|:::..|...|. :.| .:.......||..
beta2           137 SPFKYQSLLTKNKARVIILMVWIVSGLISFLPIQMHWYRATHQEAINCYA     186

A2B             157 P---WDGTTNESCCLVKCLFENVVPMSYMV--YFNFFGCVLPPLLIMLVI     201
                    .  .|..||::..:...:....||:..||  |...|......|..:...
beta2           187 NETCCDFFTNQAYAIASSIVSFYVPLVIMVFVYSRVFQEAKRQLQKIDKS     236

A2B             202 YIKIFLVACRQLQRTELMDH----SRTTLQREIHAAKSLAMIVGIFALCW     247
                    ..:..:....|:::.....|    |.....:|..|.|:|..:|:|.|.|||
beta2           237 EGRFHVQNLSQVEQDGRTGHGLRRSSKFCLKEHKALKTLGIIMGTFTLCW     286

A2B             248 LPVHAVNCVTLFQPAQGKNKPKWAMNMAILLSHANSVVNPIVYAYRNRDF     297
                    ||...||.|.:.|....:.:....:|.   :.:.||..||::|. |:.||
beta2           287 LPFFIVNIVHVIQDNLIRKEVYILLNW---IGYVNSGFNPLIYC-RSPDF     332

A2B             298 RYTFHKII    305
                    |..|.:::
beta2           333 RIAFQELL    340
```

B

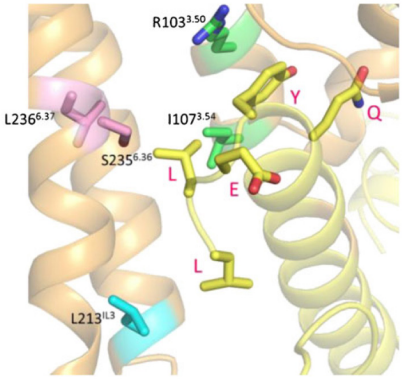

C

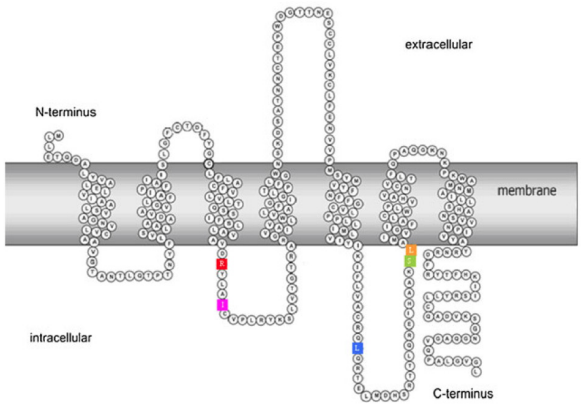

Fig. 2 (A) Sequence alignment (most similar regions only) between the $hA_{2B}R$ (A_{2B}; uniprot: P29275) and the $h\beta_2AR$ (beta2; uniprot:P07550). Conserved residues are shown as | between the two sequences. (B) A hA_{2B} Receptor/ G_s protein homology model was generated from the crystal structure of the β_2AR in contact with the $G_{\alpha s}$ protein[23] (PDB: 3SN6) to predict amino acids interacting with $G_{\alpha s}$. The last five C-terminal residues of mammalian $G_{\alpha s}$ subunit are $QYELL^{COOH}$, shown in red. (C) Snake plot of the $hA_{2B}R$. Five residues ($R103^{3.50}$, $I107^{3.54}$, $L213^{IL3}$, $S235^{6.36}$ and $L236^{6.37}$) were selected to be individually mutated to alanine based on the homology model in B).

The L213 ^{IL3}A mutant improved coupling efficiency in all yeast strains compared to the wild-type receptor, but to a different extent. The highest coupling efficiency was found in MMY28($G_{\alpha s}$) and MMY19($G_{\alpha 12}$) with a 10-fold decrease of NECA's EC_{50} values compared to the wild-type receptor in the same strain. This mutant receptor was also able to reach maximal activation levels in each yeast strain upon activation by NECA except in MMY14($G_{\alpha q}$) with a somewhat reduced E_{max} value of 76%.

The S235$^{6.36}$A mutant receptor showed the most divergent humanized G protein coupling profile. In MMY12 ($G_{\alpha WT}$) and MMY20($G_{\alpha 13}$), this mutant did not alter activation compared to the wild-type receptor in the same strain. However, it showed the largest increase of activation in MMY28($G_{\alpha s}$) with a one log-unit shift for the full agonist NECA's EC_{50}, and a 0.3-fold shift in MMY 23($G_{\alpha i1}$) (Table 2). In contrast, this mutant showed a decrease of activation in MMY24($G_{\alpha i3}$), MMY14($G_{\alpha q}$) and MMY21($G_{\alpha 14}$) (up to 3.1-fold in MMY21, Table 2) and a complete loss of activation was observed in MMY19($G_{\alpha 12}$). S235$^{6.36}$A was only able to reach near-maximal activation levels in MMY24($G_{\alpha i3}$) and MMY28($G_{\alpha s}$) strains. In other strains only a partial NECA response of approx. 80% was observed, except for MMY14($G_{\alpha q}$) (50%) and MMY19($G_{\alpha 12}$) (no activation) (Table 2).

L236$^{6.37}$A showed a decreased response to NECA in the magnitude of 1.3-fold to 21-fold in all yeast strains compared to the wild-type receptor in the same strain (Table 2). L236$^{6.37}$A reached near-maximal activation levels in most strains except for MMY19 (50%), MMY14 (83%) and MMY20 (85%). Interestingly, L236$^{6.37}$A also induced less constitutive activity in MMY28 than other receptors (wild-type and mutated) in this strain (data not shown).

Table 2. EC_{50}, fold of EC_{50} and E_{max} values of wild-type and mutant A_{2B} receptors in all examined MMY strains. The fold shift of EC_{50} was calculated by dividing the EC_{50} of the mutant receptor by the EC_{50} of the wild-type receptor of the same strain. $\%E_{max}$ represents the intrinsic activity of the receptor, where the mean maximal growth level of MMY12 carrying wild-type receptor in response to the agonist NECA (10^{-4}M) was set as 100%. Results were mostly obtained from two independent experiments, performed in duplicate (individual values in parentheses).

		EC_{50}	fold EC_{50}	% E_{max}
MMY 12	Wild-type	393 ± 92	1	100 ± 3
($G_{\alpha WT}$)	$R103^{3.50}A$	-	-	13 (17, 9)
	$I107^{3.54}A$	-	-	0 (0, 1)
	$L213^{IL3}A$	236 (152, 319)	0.6	100 (104, 96)
	$S235^{6.36}A$	384 (309, 459)	1	85 (83, 87)
	$L236^{6.37}A$	3099 (2503, 3694)	7.9	102 (109, 96)
MMY 14	Wild-type	1641 ± 552	1	99 ± 3
($G_{\alpha q}$)	$R103^{3.50}A$	-	-	1 (1, 1)
	$I107^{3.54}A$	-	-	(0, 0)
	$L213^{IL3}A$	483 (461, 504)	0.3	76 (75, 77)
	$S235^{6.36}A$	3109 (2102, 4115)	1.9	50 (48, 51)
	$L236^{6.37}A$	7069 (9827, 4310)	4.3	83 (83, 82)
MMY 19	Wild-type	2843 ± 1141	1	91 ± 8
($G_{\alpha 12}$)	$R103^{3.50}A$	-	-	2 (2, 1)
	$I107^{3.54}A$	-	-	1 (0, 1)
	$L213^{IL3}A$	272 (199, 345)	0.1	100 (100, 99)
	$S235^{6.36}A$	-	-	19 (8, 31)
	$L236^{6.37}A$	-	-	50 (60, 40)
MMY 20	Wild-type	384 ± 158	1	99 ± 7
($G_{\alpha 13}$)	$R103^{3.50}A$	-	-	6 (10, 2)
	$I107^{3.54}A$	-	-	3 (3, 3)
	$L213^{IL3}A$	90 (42, 137)	0.2	102 (107, 97)
	$S235^{6.36}A$	437 (501, 372)	1.1	77 (75, 80)
	$L236^{6.37}A$	5375 (4700, 6050)	14	85 (87, 84)
MMY 21	Wild-type	212 ± 91	1	108 ± 7
($G_{\alpha 14}$)	$R103^{3.50}A$	-	-	4 (5, 2)
	$I107^{3.54}A$	-	-	1 (0, 1)
	$L213^{IL3}A$	34 (17, 51)	0.2	107 (108, 106)
	$S235^{6.36}A$	664 (552, 776)	3.1	80 (78, 82)
	$L236^{6.37}A$	1335 (783, 1887)	6.3	99 (104, 94)
MMY 23	Wild-type	305 ± 137	1	91 ± 8
($G_{\alpha i1}$)	$R103^{3.50}A$	-	-	9 (15, 3)
	$I107^{3.54}A$	7629 (9162, 6095)	25	37 (38, 37)
	$L213^{IL3}A$	108 (72, 143)	0.4	95 (96, 94)
	$S235^{6.36}A$	84 (103, 65)	0.3	82 (76, 88)
	$L236^{6.37}A$	411 (398, 424)	1.3	98 (102, 95)
MMY 24	Wild-type	59 ± 10	1	113 ± 5
($G_{\alpha i3}$)	$R103^{3.50}A$	-	-	9 (7, 10)
	$I107^{3.54}A$	-	-	2 (2, 1)
	$L213^{IL3}A$	49 (25, 72)	0.8	104 (113, 96)
	$S235^{6.36}A$	175 (174, 176)	3	105 (109, 102)
	$L236^{6.37}A$	680 (504, 855)	11.6	112 (121, 103)
MMY 28	Wild-type	25 ± 6	1	112 ± 4
($G_{\alpha s}$)	$R103^{3.50}A$	57 (53, 61)	2.2	95 (98, 92)
	$I107^{3.54}A$	47 (25, 69)	1.9	103 (100, 106)
	$L213^{IL3}A$	23 (31, 15)	0.9	105 (104, 106)
	$S235^{6.36}A$	33 (42, 24)	1.3	105 (110, 100)
	$L236^{6.37}A$	538 (755, 321)	21	96 (95, 98)

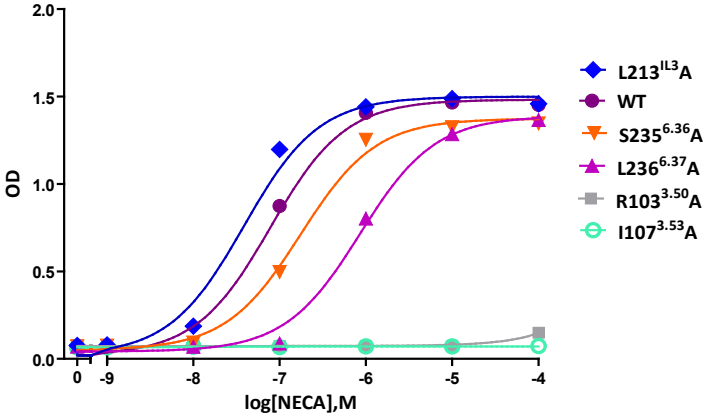

Fig. 3 Concentration-effect curves from liquid assay experiments. Curves are shown of the wild-type, and five mutant receptors L213 ^{IL3}A, S235$^{6.36}$A, L236$^{6.37}$A, R103$^{3.50}$A and I107$^{3.53}$A in the MMY24($G_{\alpha i3}$) strain responding to the adenosine receptor agonist NECA. The assay was performed in YNB-ULH medium.

Determination of expression level of the $hA_{2B}R$ in different yeast strains

In Figure 4A a Western blot analysis of the expression levels of the WT $hA_{2B}R$ and three mutants is shown. In each gel the antibody used recognized the top and bottom bands as specific bands of the $hA_{2B}R$ while the middle one was used as a reference band, since it is not specific for the receptor as evidenced by the MMY12 strain carrying the plasmid pDT-PGK without receptor. Quantitative bar graphs derived from the data in Figure 4A are shown in Figure 4B. Expression levels of the wild-type receptor in most strains were quite comparable (Fig. 4B). Even though mutants R103A and I107 did not respond to NECA in the liquid assay experiments, they did express in all yeast strains, except for MMY21_ I107A (Fig. 4B). These data confirm that the transformation protocols used led to robust receptor expression in (almost) all cases and, hence, provide further proof of the validity of the activation profiles established. Moreover, it seems a certain degree of receptor expression is sufficient for receptor activation. As an example, the density of the L213 ^{IL3}A mutant was lowest in MMY24 and highest in MMY28. Nevertheless, EC_{50} and E_{max} values for NECA were the virtually the same in both strains. To save costly (and commercially unavailable) antibody we did not screen S235A and L236A mutant receptors, since their transferred strains always showed NECA conentration-response curves with high E_{max} values.

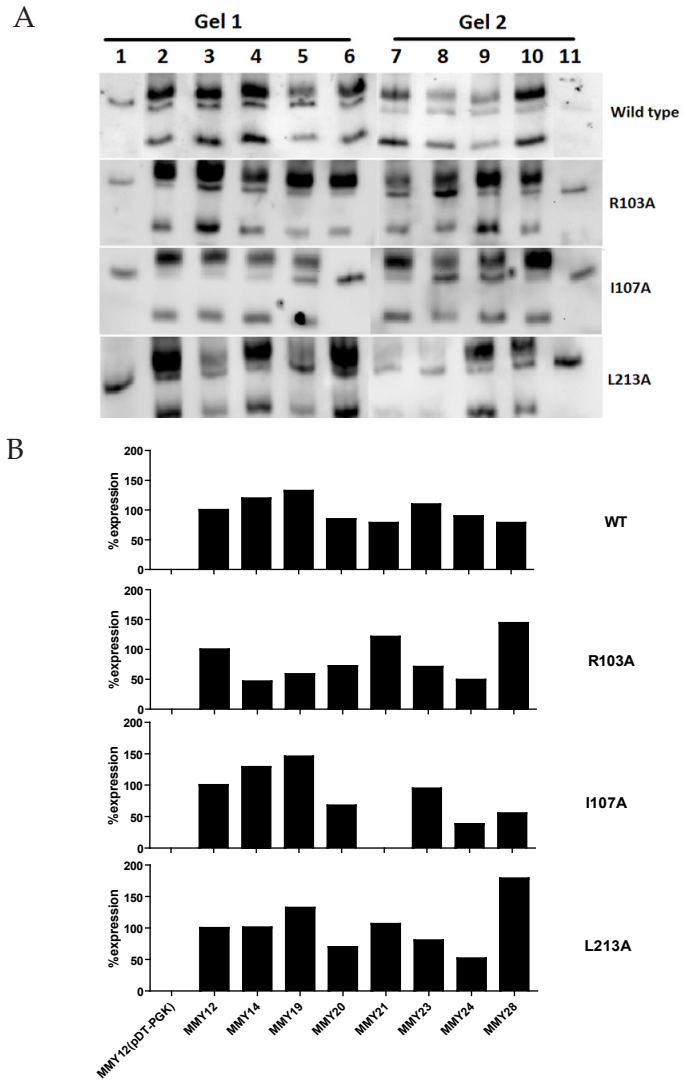

Fig. 4 Western blot analysis of the wild-type $hA_{2B}R$ and R103A, I107A and L213A mutations from top to bottom panel as expressed in different MMY strains. (A) Gel 1: Lane 1, MMY12 carrying pDT-PGK without receptor; Lane 2- 6, MMY12, MMY14, MMY19, MMY20 and MMY21 carrying pDT-PGK_A_{2B} wild-type or mutant receptor. Gel 2: Lane7-10, MMY23, MMY24, MMY28 and MMY12 carrying pDT-PGK_A_{2B} mutant receptor; Lane 11, MMY12 carrying pDT-PGK without receptor. The A_{2B} receptor specific bands are 29 kD and 50 kD, which are absent in MMY12 carrying pDT-PGK without receptor; Nonspecific band at approx. 45 kDa was used as loading control, which also appeared in MMY12 carrying pDT-PGK without receptor. (B) Bar graphs were calculated from a densitometric analysis of the blots. The ratio was determined between the density of the specific bands and that of the nonspecific band that is always present on the blots. MMY12 carrying wild-type or mutant receptor was set as 100% and MMY12 carrying the empty vector pDT-PGK without receptor was set as 0%.

Ligand binding assay of wild-type and mutant $hA_{2B}R$ expressed in MMY24($G_{\alpha i3}$)

To investigate whether the binding affinity of NECA was changed in the mutated receptors, we performed a number of radioligand binding experiments. Traditionally, this assay is cumbersome in yeast cells, but we managed to obtain sufficient levels of specific [^{3}H]PSB-603 binding to do displacement assays on wild-type, L213A and L236A receptors. The two mutant receptors had a similar IC_{50} value for NECA displacing [^{3}H]PSB-603 binding compared to the wild-type receptor (Table 3). However, the binding affinity of the radiolabeled antagonist for the other mutants, R103A, I107A and S235A, appeared to be decreased. As a consequence we did not obtain a high enough window of specific [^{3}H]PSB-603 binding to perform a radioligand displacement assay.

Table 3. Radioligand binding experiments of wild-type and mutant hA_{2B} receptors expressed in MMY24($G_{\alpha i3}$) using 1.5 nM [^{3}H]PSB-603. Specific binding of wild-type receptor was set at 100%. IC_{50} values were obtained from competition binding curves of five independent experiments, performed in duplicate.

Mutant	% specific binding	IC_{50}(μM)
Wild-type	100	1.85 ± 0.87
R103A	0	nd
I107A	12	nd
L213A	94	1.90 ± 1.64
S235A	20	nd
L236A	158	1.88 ± 0.6

nd: not determined

Discussion

Even though the mechanisms of interaction between GPCRs and their G proteins are largely unknown, the α4-helix and α4-β6 loop[34, 35], the N-terminus[36] and C-terminus of G_α subunits[37] have been described to be important for GPCR-G_α protein binding and selectivity. Of those the C-terminus of the G_α subunit appears most intimately involved in binding the receptor. This was already evident from available crystal structures[23, 30] and further confirmed in molecular dynamics

calculations by Kling et al., to show that three residues at the C-terminus of $G_{\alpha s}$ are in close contact with at least 5 amino acids of the β_2AR[38]. In the present study, we examined the mechanism of interaction between the A_{2B} receptor and the last five amino acid residues in the C-terminus of G_α subunits using a functional yeast system combined with homology modeling and mutagenesis experiments.

G protein-coupling profiles of the wild-type A_{2B} receptor

We found that the wild-type hA_{2B}R can activate many humanized G protein pathways, which is consistent with earlier findings by Brown et al. that the hA_{2B}R is quite promiscuous as it recognizes most strains with a similar rank order of activation[19]. These strains possess different humanized G proteins, in which the last five amino acid residues of the endogenous Gpa1p C-terminal have been replaced with the same sequence from mammalian G_α proteins, covering the four major classes: $G_{\alpha i}$, $G_{\alpha s}$, $G_{\alpha q}$ and $G_{\alpha 12}$. It is worth noting that the differences in activation profiles found in the present study can only be due to the variation in the five terminal amino acids of the humanized C-terminus of the G_α subunit. This has the advantage of providing a detailed snapshot of G protein activation without confounding factors such as further differences in the composition of the various G_α subunits.

The A_{2B} receptor is preferentially coupled to the G_s pathway and to a lesser degree to the G_q pathway in many cells[39], and these two G proteins also couple well in our yeast system (*S. cerevisiae* strains MMY28($G_{\alpha s}$), MMY14($G_{\alpha q}$) and MMY21($G_{\alpha 14/q}$), respectively). Interestingly, the receptor appears to couple well to two strains with a $G_{\alpha i}$ protein, MMY24($G_{\alpha i3}$) and MMY23($G_{\alpha i1}$), too, providing proof of the promiscuity mentioned above. However, this is not a "general" GPCR feature. For instance, Stewart et al used the same yeast system to study functional selectivity of agonists and antagonists of the adenosine A_1 receptor and learned that only the $G_{i/o}$ pathway was addressed[18]. Likewise, the hydroxy-carboxylic acid receptor HCA_3 can only activate the G_i pathway through its agonist acifran (preliminary data not shown).

G protein-coupling profiles of mutants of the $hA_{2B}R$

In the present study we sought to identify amino acid residues on the $hA_{2B}R$ that are vital in G protein coupling. The β_2AR-G_s crystal structure (PDB: 3SN6) was chosen as the template to predict such amino acids in the $hA_{2B}R$. $R103^{3.50}$, $I107^{3.54}$, $L213^{IL3}$, $S235^{6.36}$ and $L236^{6.37}$ were selected to be mutated into alanine because they are interacting with the last five amino acids of the $G_{\alpha s}$ protein in the β_2AR-G_s crystal structure. We will discuss these five amino acids in the light of our findings.

Residues $R103^{3.50}$ and $I107^{3.54}$

These two residues ($R103^{3.50}$ and $I107^{3.54}$) are located on the intracellular side of TM3 and are included in the consensus sequence (I/L)*XX*D$R^{3.50}$Y*XX*(I/V)$^{3.54}$[32]. $R^{3.50}$ is a part of the most conserved motif in the class A GPCRs: Asp-Arg-Tyr (DRY). This arginine is 100% conserved within the subfamily of adenosine receptors and nucleotide-like receptors, and 97% of all Class A rhodopsin-like receptors. This is less so for $I^{3.54}$ with 54% overall conservation (Table 4).

Not surprisingly $R^{3.50}$ has been the subject of many mutation studies, exemplified by their high occurrence in the GPCRDB mutation database[40]. The DRY-motif is part of a so-called "ionic lock"[41, 42], consisting of a number of interactions between the DRY-motif and amino acids in TM6; the interaction that is most prominent is the interaction between $R^{3.50}$ and a negatively charged residue in TM6, Asp (D) or Glu (E). These interactions are thought to stabilize the receptor in an inactive conformation and thereby decrease its basal activity[43]. When the receptor is activated the ionic lock is broken and TM6 is moving outward. Breaking the ionic look through mutation might thus lead to constitutive activity, which was shown to be the case on the adenosine A_3 receptor[44]. While this mechanism seems to hold true for some receptors it does not hold for every GPCR, as on the histamine H_4 receptor[45]. $R^{3.50}$ in this case turned out to be very important for G protein coupling. Our own results comply with data found for the α_{1b}-adrenergic receptor where mutations of $R^{3.50}$ resulted in a complete loss of receptor-mediated response in the majority of mutant receptors[46].

It has been proposed that there are many other conserved residues that help $R^{3.50}$ switch the receptor on or off, such as $D^{3.49}$ and $I/V^{3.54}$[32]. The latter position (3.54) is always conserved with a bulky β-branched, hydrophobic residue (Val or Ile). A mutagenesis study in the gonadotropin-releasing hormone (GnRH) receptor offered a hypothesis as to why there is a lack of receptor signaling in a receptor with a mutated $I^{3.54}$. According to Ballesteros et al. $I^{3.46}$, $A^{3.49}$, and $I^{3.54}$, all highly conserved amino acids, form a layer around $R^{3.50}$, the so-called arginine-cage motif. $I^{3.54}A$ mutations caused significant reductions in receptor signaling efficacy and reduced the affinity for GnRH as well. In the WT receptor the bulky side chain of $I^{3.54}$ cannot move much as it readily clashes with the side chain of $R^{3.50}$. This does not occur in the $I^{3.54}A$ mutant, which allows $R^{3.50}$ to take an unfavorable conformation with an orientation to the aqueous cytoplasm. This might prevent $R^{3.50}$ from taking part in receptor activation. Thus the purpose of $I^{3.54}$ appears to be a defined and strictly controlled positioning of $R^{3.50}$[32].

The results from our yeast screening assay add a layer of detail to these general findings, in that some G proteins seem more affected than others. We found that mutation to alanine of $R103^{3.50}$and $I107^{3.54}$ in the $hA_{2B}R$ abolished many humanized G protein pathways (Table 2) and, hence, we concluded they are very important for interaction with humanized G proteins. $R103^{3.50}$ is crucial for each pathway, except for $G_{\alpha s}$, whereas $I107^{3.54}$ is vital for most G protein pathways as well, although after mutation some interaction remained with both $G_{\alpha i1}$ and $G_{\alpha s}$.

Table 4. Sequence conservation of the four helical amino acids involved in G protein interaction, among adenosine receptors, nucleotide-like receptors*, and class A rhodopsin-like receptors as found on GMOS (GPCRs Motif Searcher, http://lmc.uab.cat/gmos/).

Amino acid in A_{2B}	Conservation in Adenosine receptors	Most occurring	Conservation in Nucleotide-like receptors	Most occurring	Conservation in Class A rhodopsin-like receptors	Most occurring
$R103^{3.50}$	100.0%	R - 100%	100.0%	R - 100%	96.98%	R - 96.98%
$I107^{3.54}$	35.29%	V - 64.70%	41.74%	V - 46.60%	53.68%	I - 53.68%
$S235^{6.36}$	85.29%	S - 85.29%	33.00%	S - 33.00%	2.81%	T - 32.25%
$L236^{6.37}$	85.29%	L - 85.29%	36.89%	L - 36.89%	38.59%	L - 38.59%

* Nucleotide-like receptors: adenosine A_1, A_{2A}, A_{2B}, A_3 receptors; P2RY1, 4, 5, 6, 8, 9, 10, 11; GPR23, 35, 91, 92, 174.

Other three residues $L213^{IL3}$, $S235^{6.36}$ and $L236^{6.37}$

Even though the investigated mutants only have one residue altered at the time, they show substantial differences in ligand activation of the receptor. A prominent enhancement was seen with the $L213^{IL3}A$ mutant; in all cases/strains NECA was more active than on the wild-type receptor, particularly in MMY19($G_{\alpha 12}$), with a 10-fold increase in potency. This result shows once more the dependency of agonist potency on amino acids other than those in the ligand binding site, and may even shed light on pharmacological principles such as receptor reserve. Apparently, the leucine on position 213 in the wild-type receptor acts as a deactivating switch.

The role of $S^{3.36}$ seems to be somewhat more ambiguous. This residue when mutated to alanine caused mostly a decrease of receptor signaling. $S^{6.36}$ is much conserved (Table 4) within the adenosine receptor subfamily (85%), but less so in the nucleotide-like receptors (33%) and hardly in all class A rhodopsin-like receptors (2.8%). Several mutations have been made in different receptors on the 6.36 position but none of the original amino acids was a serine. The closest mutation is a $T^{6.36}A$ in the human muscarinic acetylcholine M1 receptor where the mutant did not significantly differ from wild-type in PI turnover[47]. In the present study, the $S2^{6.36}A$ mutation showed a most divergent G protein profile: improved activation efficiency in MMY28($G_{\alpha s}$) and MMY23($G_{\alpha i1}$); no change in

MMY20($G_{\alpha i3}$) similar to MMY12($G_{\alpha WT}$); decreased activation in MMY14($G_{\alpha q}$), MMY24($G_{\alpha i3}$), MMY21($G_{\alpha 14}$) and a complete loss of activation in MMY19($G_{\alpha 12}$) (Table 2). Apparently the change from a hydrophilic (serine) to a hydrophobic (alanine) amino acid is dealt with differently by the G proteins studied.

$L^{6.37}$ is quite conserved: 85% in adenosine receptors, 37% in nucleotide-like receptors, and 39% in all class A rhodopsin-like receptors. In the A_{2A} receptor the $L^{6.37}A$ mutation along with several others was used to provide receptor thermostabilization for crystallographic purposes[48]. The mutant caused no effect on ligand pharmacology. In our hands, the $L236^{6.37}A$ mutation decreased activation in all humanized G protein pathways, most outspoken for MMY28. Apparently, the leucine residue is vital for G protein interaction and activation.

Function of hydroxyl-group at C-terminus of G_{α} subunits for wild-type $hA_{2B}R$

The slight differences in amino acid composition in some of the G_{α} subunits allow an almost atomic dissection of the observed effects. There is an 8-fold potency difference of NECA in the two G_q pathway strains MMY21($G_{\alpha 14}$) with an EC_{50} value of 212 nM and MMY14($G_{\alpha q}$) with an EC_{50} value of 1641 nM. Both have the same amino acid residues at the C-terminus of the G_{α} protein except for the fourth residue position counting from the end of the C-terminus with a tyrosine in MMY14 and a phenylalanine in MMY21 (Table 1). The only difference between tyrosine and phenylalanine is a hydroxyl-group, which leads to the large decrease in potency for NECA. However, there is an opposite phenomenon at the last amino acid of the C-terminus between two $G_{\alpha i}$ pathway strains, MMY24($G_{\alpha i3}$) and MMY23($G_{\alpha i1}$). A tyrosine as last amino acid of the end of the C-terminus position of MMY24 yielded an EC_{50} value of 59 nM for NECA, whereas the phenylalanine on the same position in MMY23 gave an EC_{50} value of 305 nM (Tables 1 and 2). This particular tyrosine hydroxyl-group is apparently enough to decrease the EC_{50} value by 6-fold, which is equivalent to an increase of activation and NECA potency. Taken together, subtle changes such as the presence or absence of a hydroxyl-group located in the C-terminus of the G_{α} protein control activation of GPCRs.

Concluding remarks

We reported on a yeast system that is very well suited for the study of a G protein-coupled receptor (the $hA_{2B}R$ in this case), its activation and its G protein preference. This highly efficient and inexpensive screening system was used to map residues at the cytoplasmic side of the receptor and in the C-terminus of different G_{α} subunits important for receptor activation. The results provided detailed information about receptor/G protein binding and G protein selectivity.

Acknowledgements

Rongfang Liu thanks the China Scholarship Council (CSC) for her PhD scholarship. NWO provided a TOP grant to A.P. IJ. (714.011.001). The authors are grateful to Prof C.E. Müeller of Bonn University for the generous gift of [^{3}H] PSB-603 and to Simon Dowell from GSK for providing the yeast strains and experimental protocols.

References

[1] Oldham, W.M., et al. *Mechanism of the receptor-catalyzed activation of heterotrimeric G proteins.* Nat. Struct. Mol. Biol. (2006) 13: 772-777.

[2] Baltoumas, F.A., et al. *Interactions of the alpha-subunits of heterotrimeric G-proteins with GPCRs, effectors and RGS proteins: A critical review and analysis of interacting surfaces, conformational shifts, structural diversity and electrostatic potentials.* J. Struct. Biol. (2013) 182: 209–218.

[3] Fredholm, B.B., et al. *Structure and function of adenosine receptors and their genes.* Naunyn-Schmiedeberg's Arch. Pharmacol. (2000) 362: 364-374.

[4] Fredholm, B.B., et al. *Comparison of the potency of adenosine as an agonist at human adenosine receptors expressed in Chinese hamster ovary cells.* Biochem. Pharmacol. (2001) 61: 443-448.

[5] Wei, W., et al. *Blocking A_{2B} adenosine receptor alleviates pathogenesis of experimental autoimmune encephalomyelitis via inhibition of IL-6 production and Th17 differentiation.* J. Immunol. (2013) 190: 138-146.

[6] Wei, Q., et al. *A_{2B} adenosine receptor blockade inhibits growth of prostate cancer cells.* Purinergic Signal. (2013) 1-10.

[7] Stagg, J., et al. *Anti-CD73 antibody therapy inhibits breast tumor growth and metastasis.*

Proc. Natl. Acad. Sci. (2010) 107: 1547-1552.

[8] Owen, S.J., et al. *Loss of adenosine A_{2B} receptor mediated relaxant responses in the aged female rat bladder; effects of dietary phytoestrogens.* Naunyn-Schmiedeberg's Arch. Pharmacol. (2012) 385: 539-549.

[9] Cekic, C., et al. *Adenosine A_{2B} receptor blockade slows growth of bladder and breast tumors.* J. Immunol. (2012) 188: 198-205.

[10] Koscsó, B., et al. *Stimulation of A_{2B} adenosine receptors protects against trauma–hemorrhagic shock-induced lung injury.* Purinergic Signal. (2013) 1-6.

[11] Bot, I., et al. *Adenosine A_{2B} receptor agonism inhibits neointimal lesion development after arterial injury in apolipoprotein E–deficient mice.* Arterioscler. Thromb. Vasc. Biol. (2012) 32: 2197-2205.

[12] Pausch, M.H. *G-protein-coupled receptors in Saccharomyces cerevisiae: high-throughput screening assays for drug discovery.* Trends Biotechnol. (1997) 15: 487-494.

[13] Peeters, M.C., et al. *Three "hotspots" important for adenosine A_{2B} receptor activation: a mutational analysis of transmembrane domains 4 and 5 and the second extracellular loop.* Purinergic Signal. (2011) 1-16.

[14] Mathew, E., et al. *Functional fusions of T4 lysozyme in the third intracellular loop of a G protein-coupled receptor identified by a random screening approach in yeast.* Protein Eng. Des. Sel. (2013) 26: 59-71.

[15] Jaeschke, H., et al. *Preferences of transmembrane helices for cooperative amplification of $G_{\alpha s}$ and $G_{\alpha q}$ signaling of the thyrotropin receptor.* Cell. Mol. Life Sci. (2008) 65: 4028-4038.

[16] Evans, B.J., et al. *Expression of CXCR4, a G-protein–coupled receptor for CXCL12 in Yeast: identification of new-generation inverse agonists.* Methods Enzymol. (2009) 460: 399-412.

[17] Minic, J., et al. *Yeast system as a screening tool for pharmacological assessment of G protein coupled receptors.* Curr. Med. Chem. (2005) 12: 961-969.

[18] Stewart, G.D., et al. *Determination of adenosine A_1 receptor agonist and antagonist pharmacology using Saccharomyces cerevisiae: implications for ligand screening and functional selectivity.* J. Pharm. Exp. Ther. (2009) 331: 277-286.

[19] Brown, A.J., et al. *Functional coupling of mammalian receptors to the yeast mating pathway using novel yeast/mammalian G protein α subunit chimeras.* Yeast (2000) 16: 11-22.

[20] Dowell, S.J. and Brown, A.J. *Yeast assays for G protein-coupled receptors.* Methods Mol. Biol. (2009) 552: 213-229.

[21] Dowell, S.J. *Yeast assays for G-protein–coupled receptors.* Receptors Channels (2002) 8: 343-352.

[22] Cardozo, T., et al. *Homology modeling by the ICM method.* Proteins: Struct., Funct., Bioinf. (2004) 23: 403-414.

[23] Rasmussen, S.G., et al. *Crystal structure of the β_2 adrenergic receptor-G_s protein complex.* Nature (2011) 477: 549-555.

[24] DeLano, D.W., *The PyMOL Molecular Graphics System, Version 1.5. 0.4 Schrödinger, LLC.*

[25] Gietz, D., et al. *Improved method for high efficiency transformation of intact yeast cells.*

Nucleic Acids Res. (1992) 20: 1425.

[26] Li, Q., et al. *ZM241385, DPCPX, MRS1706 are inverse agonists with different relative intrinsic efficacies on constitutively active mutants of the human adenosine A_{2B} receptor.* J. Pharmacol. Exp. Ther. (2007) 320: 637-645.

[27] Feoktistov, I., et al. *Immunological characterization of A_{2B} adenosine receptors in human mast cells.* Drug Dev. Res. (2003) 58: 461-471.

[28] Peeters, M., et al. *The role of the second and third extracellular loops of the adenosine A_1 receptor in activation and allosteric modulation.* Biochem. Pharmacol. (2012) 84: 76-87.

[29] Venkatakrishnan, A., et al. *Molecular signatures of G-protein-coupled receptors.* Nature (2013) 494: 185-194.

[30] Scheerer, P., et al. *Crystal structure of opsin in its G-protein-interacting conformation.* Nature (2008) 455: 497-502.

[31] Fredholm, B.B., et al. *International union of basic and clinical pharmacology. LXXXI. nomenclature and classification of adenosine receptors an update.* Pharmacol. Rev. (2011) 63: 1-34.

[32] Ballesteros, J., et al. *Functional microdomains in G-protein-coupled receptors the conserved arginine-cage motif in the gonadotropin-releasing hormone receptor.* J. Biol. Chem. (1998) 273: 10445-10453.

[33] Ballesteros, J.A. and Weinstein, H. *Integrated methods for the construction of three-dimensional models and computational probing of structure-function relations in G protein-coupled receptors.* Methods Neurosci. (1995) 25: 366-428.

[34] Bae, H., et al. *Two amino acids within the α4 helix of $G_{\alpha i1}$ mediate coupling with 5-hydroxytryptamine 1B receptors.* J. Biol. Chem. (1999) 274: 14963-14971.

[35] Bae, H., et al. *Molecular determinants of selectivity in 5-hydroxytryptamine1B receptor-G protein interactions.* J. Biol. Chem. (1997) 272: 32071-32077.

[36] Taylor, J.M., et al. *Binding of an alpha 2 adrenergic receptor third intracellular loop peptide to G beta and the amino terminus of G alpha.* J. Biol. Chem. (1994) 269: 27618-27624.

[37] Blahos, J., et al. *Extreme C terminus of G protein α-subunits contains a site that discriminates between G_i-coupled metabotropic glutamate receptors.* J. Biol. Chem. (1998) 273: 25765-25769.

[38] Kling, R.C., et al. *Active-state models of ternary GPCR complexes: determinants of selective receptor-G-protein coupling.* PLOS ONE (2013) 8: e67244.

[39] Thimm, D., et al. *Ligand-specific binding and activation of the human adenosine A_{2B} receptor.* Biochemistry (2013) 52: 726-740.

[40] Vroling, B., et al. *GPCRDB: information system for G protein-coupled receptors.* Nucleic Acids Res. (2011) 39: D309-D319.

[41] Vogel, R., et al. *Functional role of the "ionic lock"—an interhelical hydrogen-bond network in family A heptahelical receptors.* J. Mol. Biol. (2008) 380: 648-655.

[42] Scheer, A., et al. *Constitutively active mutants of the alpha 1B-adrenergic receptor: role of highly conserved polar amino acids in receptor activation.* EMBO J. (1996) 15: 3566.

[43] Flanagan, C.A. *A GPCR that is not "DRY".* Mol. Pharmacol. (2005) 68: 1-3.

[44] Chen, A., et al. *Constitutive activation of A_3 adenosine receptors by site-directed mutagenesis.* Biochem. Biophys. Res. Commun. (2001) 284: 596-601.

[45] Schneider, E.H., et al. *Impact of the DRY motif and the missing "ionic lock" on constitutive activity and G-protein coupling of the human histamine H4 receptor.* J. Pharmacol. Exp. Ther. (2010) 333: 382-392.

[46] Scheer, A., et al. *Mutational analysis of the highly conserved arginine within the Glu/Asp-Arg-Tyr motif of the α1b-adrenergic receptor: effects on receptor isomerization and activation.* Mol. Pharmacol. (2000) 57: 219-231.

[47] Högger, P., et al. *Activating and inactivating mutations in N-and C-terminal i3 loop junctions of muscarinic acetylcholine Hm1 receptors.* J. Biol. Chem. (1995) 270: 7405-7410.

[48] Doré, A.S., et al. *Structure of the adenosine A_{2A} aeceptor in complex with ZM241385 and the Xanthines XAC and Caffeine.* Structure (2011) 19: 1283-1293.

[49] Simon, M.I., et al. *Diversity of G proteins in signal transduction.* Science (1991) 252: 802-808.